Available online at www.sciencedirect.com

SciVerse ScienceDirect

Ceramics International 39 (2013) 7735–7741

CERAMICS INTERNATIONAL

www.elsevier.com/locate/ceramint

Influence of initial pH on the microstructure of $YBa_2Cu_3O_{7-x}$ superconducting thin films derived from DEA-aqueous sol–gel method

Xiao Tang*, Yue Zhao, Jean-Claude Grivel

Department of Energy Conversion and Storage, Technical University of Denmark, DK-4000 Roskilde, Denmark

Received 7 January 2013; received in revised form 7 March 2013; accepted 10 March 2013
Available online 28 March 2013

Abstract

A fluorine-free aqueous sol–gel technique was used to fabricate YBCO superconducting thin films. Acetic acid was added in order to modify the complexation process taking place between the metal cations and the organic chelating agents. The electrical resistance and the pH value were used as indicators of the quality of the precursors. When pH = 6.5, the precursor solution had the lowest resistance, implying a good ionization of the starting metal elements. By using the optimal precursor, the film was found to have very small sized particles after pyrolysis. Consequently, the annealed YBCO films are characterized by a sharp superconducting transition with a *Jc* (77 K) of 0.25 MA/cm^2.

Keywords: A. Sol-gel processes; A. Films; A. Precursors: organic; C. Superconductivity

1. Introduction

Chemical solution deposition (CSD) routes are promising for the industrialization of $YBa_2Cu_3O_{7-x}$ superconducting films owing to the low cost of the technique, which does not require any high vacuum equipment [1]. Particularly in the past decade, the trifluoroacetate metal-organic deposition (TFA-MOD) process has attracted much interest because of the resulting high critical current densities (*Jc*) and the reproducibility of the product [2]. The TFA-MOD has however two intrinsic disadvantages, one being the released hazardous HF gas as a byproduct. The other is the time-consuming decomposition process, which has been an insurmountable obstacle to fast manufacturing up-scaling [3]. Therefore, it is of high interest to develop environmentally friendly and faster CSD methods. For this reason, some non-fluorine techniques have been explored, such as the trimethylacetate-propionic acid (TMAP) process [4], the so-called advanced MOD process by using naphthenates [5], as well as sol–gel methods involving chelation between metal cations and citric acid (CA) [6] or ethylenediaminetetraacetic acid (EDTA) [7].

In this paper, an environmentally friendly water-based sol–gel method was used to synthesize YBCO superconducting films. Diethylamine (DEA) was introduced into the solution as the chelating agent in order to prevent segregation and precipitation. As shown in Table 1, compared to other standard chelating agents, one of the most important advantages of DEA is its low molecular weight, which can help suppressing the crack and pore formation during pyrolysis [8].

However, according to previous publications on sol–gel techniques for producing YBCO films, the window of the optimal pH value of the precursor solution is quite narrow [9,10]. Additionally, publications relating to the production of other functional materials through some similar sol–gel processes confirmed that precursors with different pH values can lead to various kinds of bonding behaviors within the polymeric network, which may further influence the morphology of the sintered products [11,12].

With the aim of obtaining high-quality YBCO superconducting films, we systematically investigated the effect of the pH value of the YBCO sol–gel precursor on the chelation and polymerization mechanisms. The optimization of the annealing process is discussed as well.

2. Experimental

2.1. Preparation of the samples

Precursor solution was prepared by mixing stoichiometric amounts of the metal acetates $Y(CH_3COO)_3 \cdot 4H_2O$ (Purity

*Corresponding author. Tel.: +45 50224088.
E-mail address: txia@dtu.dk (X. Tang).

0272-8842/$ - see front matter © 2013 Published by Elsevier Ltd and Techna Group S.r.l.
http://dx.doi.org/10.1016/j.ceramint.2013.03.030

Table 1
The molecular weight of some commonly used organic complexants.

Complexant	EDTA	TEA	DEA	TA	CA
Molecular weight (g mol)	292	150	105	150	192

EDTA: ethylenediaminetetraacetic acid; TEA: triethanolamine; DEA: diethanolamine; TA: Tartaric acid; CA: citric acid.

99.9%, Alfa Aesar), $Ba(CH_3COO)_2$ (Purity 99%, Alfa Aesar), and $Cu(CH_3COO)_2 \cdot H_2O$ (Purity 98%, Alfa Aesar) at the ratio of Y:Ba:Cu=1:2:3 and dissolving in deionized water. After 1 h of constant stiring at 90 °C, DEA (Purity 99%, Alfa Aesar) was added as the chelating agent to give a ratio of DEA:Metal=1.7:1, immediately yielding a dark blue solution without precipitation. After 12 h of reaction at 60 °C, excess water was removed by using a rotary evaporator until the total metal cation concentration reached 1.5 mol/l. Finally, acetic acid (Purity 99%, Alfa Aesar) was added in order to obtain solutions with different pH values. For the investigation of the thin films, selected precursor solutions were dip-coated onto 5 mm × 10 mm lanthanum aluminate $LaAlO_3$ (LAO) substrates at a withdrawing speed of 5 mm/min. Prior to coating, all the substrates were cleaned with 35.5% hydrochloric acid and pretreated at 700 °C for 5 h in pure oxygen. The coated films were dried in a furnace at 80 °C for 2 hto evaporate most of the solvent. Thereafter, the pyrolysis process was performed up to 450 °C under pure oxygen flow for 60 min in order to decompose the organic compounds present in the precursor. This coating-pyrolysis procedure was repeated to increase the film thickness. After cooling them down to room temperature, the pyrolyzed films were heated from 20 °C to 770–810 °C and held for 1 h. A mixed gas atmosphere consisting of argon with 100 ppm oxygen flowed throughout the tube furnace during the entire annealing process. After crystallization, the samples were cooled to 450 °C and held for five hours under an atmosphere of pure oxygen in order to obtain a defectless superconducting orthorhombic crystal structure. Finally, the samples were cooled down to room temperature.

2.2. Characterization of the samples

The pH value of the initial solutions was measured using a pH-meter. The resistivity and the IR spectra of the gel samples were measured by a FLUKE (8020B) multimeter and a Bruker Tensor 27 spectrometer, respectively. The morphologies of the pyrolyzed amorphous films and annealed crystallized films were observed by a DualScope atomic force microscope (AFM) and a supra 35 scanning electron microscope (SEM) from Zeiss, respectively. The microstructures of the samples were characterized using a BrukerD8 x-ray diffractometer with CuKα radiation. AC suscepitibility measurements combined with hysteresis loops were carried out in a CRYOGENIC cryogen free measuring system (CFMS). The critical current densities (*Jc*) of the samples were calculated using the extended Bean critical state model [13], for which the key parameter *t* (thickness) was measured on a F20 ellipsometer produced by Filmetrics Company.

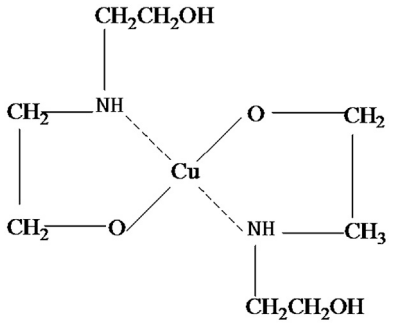

Fig. 1. Possible conformation of Cu metal ion with DEA ligands.

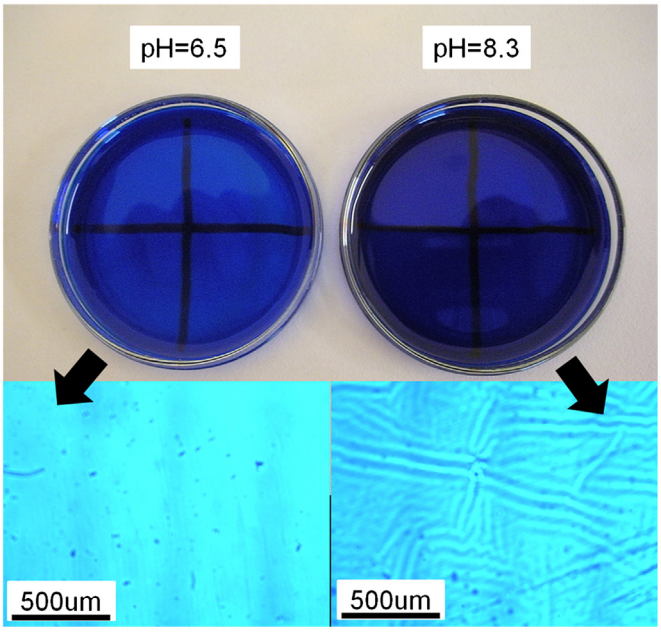

Fig. 2. Picture and OPT micrograph of the gel samples with pH=6.5 and pH=8.3.

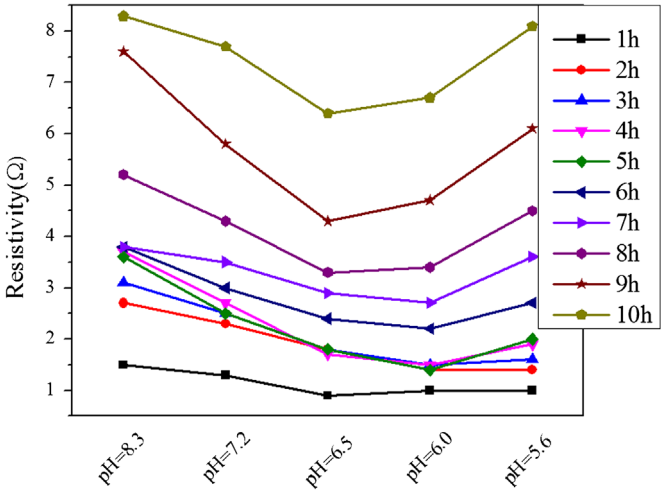

Fig. 3. Resistance evolution of the samples with different pH values as a function of evaporation time.

3. Results and discussion

In order to control the chelation–polymerization process, the pH value was carefully monitored. In the beginning, the basic idea is to suppress the hydrolysis of the metal ions by stimulating complexation with DEA ligands. In this situation, soluble chelate complexes are favored instead of the precipitation of aquo–hydroxo complexes [1]. A possible complex structure is shown in Fig. 1.

Similarly to a previous publication where the conductivity had been chosen as an index to characterize the quality of a precursor solution [14], we measured the resistance as a function of time of solution samples that were stored in open dishes of the same size, while the water slowly evaporated. Fig. 2 shows the gel samples with initial pH values of 6.5 and 8.3 after 10 h of evaporation. The different colors imply that different chelating and polymerization processes occured during evaporation.

As shown in Fig. 3, the resistance increases gradually with time. Meanwhile, the total metal concentration was progressively increasing, resulting in a rising contribution to the precursor conductivity. As a result, the rate of change of the resistance as a function of time was found to be dependent on the pH of the sample. This is because diverse crystallization or complexation phenomena occurred in the different samples. During the process, several reactions may take place in the solution, as expressed in the reaction Eqs. (A) (B) and (C), where M is the metal ion, A is the complexant, AC stands for acetic acid, n and m are the coordination numbers of M and A respectively, and z and m are the valences of M and A, respectively [1]. There is a competition between reactions (A) and (B) when a complexant is present in the solution

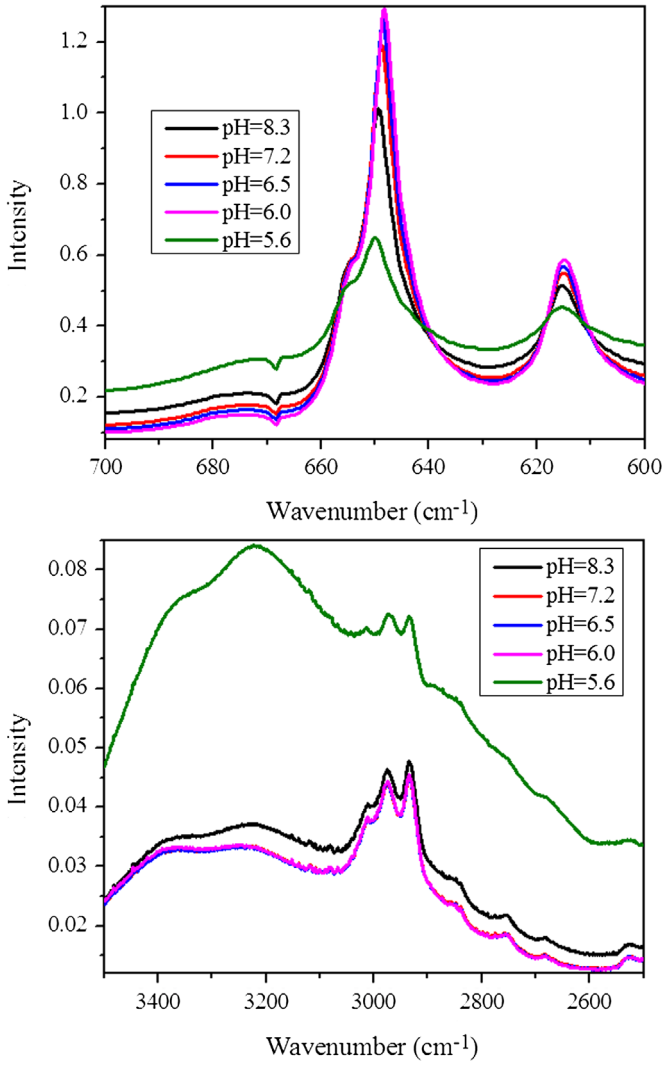

Fig. 4. FTIR spectra of the gels derived from sol samples with different pH values. Samples of pH=6.0, 6.5 and 7.2 show quite similar spectras in high wavenumber regime, thus the plots of them are overlapped.

Hydrolysis: $[M(H_2O)_n]^{z+} + hH_2O \rightarrow [M(OH)_h(H_2O)_{n-h}]^{(z-h)+} + hH_3O^+$ (A)

Complexation: $[M(H_2O)_n]^{z+} + aA^{m-} \rightarrow [M(H_2O)_w(A)_a]^{(z-am)+} + (n-w)H_2O$ (B)

Ionization: $[M(H_2O)_n](AC)_z \rightarrow [M(H_2O)_n]^{z+} + zAC^-$ (C)

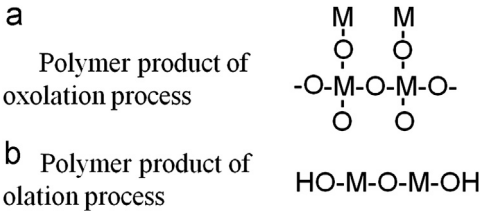

Fig. 6. Polymer products of (a) oxolation and (b) olation processes, where M is metal ion.

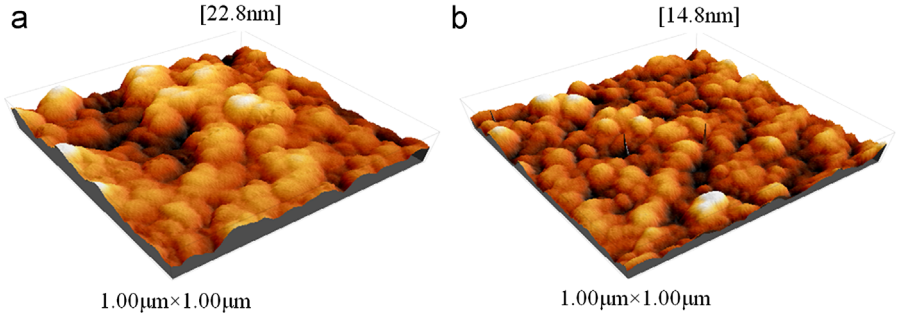

Fig. 5. AFM micrograph of the pyroplyzed films derived from the precursor of (a) pH=8.3 and (b) pH=6.5.

In the regime of high pH values, although without any precipitation, the samples were heterogeneous and highly resistive. This is due to the formation of hydroxides [$M(OH)_z$]. Previous publications proposed that the unionized hydrolyzates result from uncontrolled hydrolysis, where the reaction as shown in Eq. (A) is rapidly carried out without any interruption until all the complexed H_2O are substituted by OH^- [1,9]. With the addition of acetic acid, the pH values of the samples were approaching 6 and a minimum appears on the resistance versus pH plot around 6.5, revealing a better ionization of the metal components. This results from the complexation between the metal ions and DEA ligands, according to Eq. (B). In this process, two pentadentates were formed of one metal ion and two DEA molecules [15], rendering the metal ions well enveloped and protected from the attack of free OH^-. Also, some other reports claimed that a higher acidity of the precursor can help prevent hydrolysis of the organic metal salts [16], even without participation of a complexant. After a long-time exposure to air, samples of pH value in the range around 6.5 can transit from wet rubber to brittle polymer glass, without any loss of homogeneity. However, as the pH value decreases with the addition of acetic acid, the resistance climbed again (Fig. 3), and some white regular shaped crystals precipitated out from the solution. This phenomenon can be assigned to the re-crystallization of acetates [1,9]. With the addition of acetic acid, the concentration of AC^- is increased. Consequently the balance of Eq. (C) is shifted back to the left side and thus the ionization of $[M(H_2O)_n]$ $(AC)_z$ is undermined.

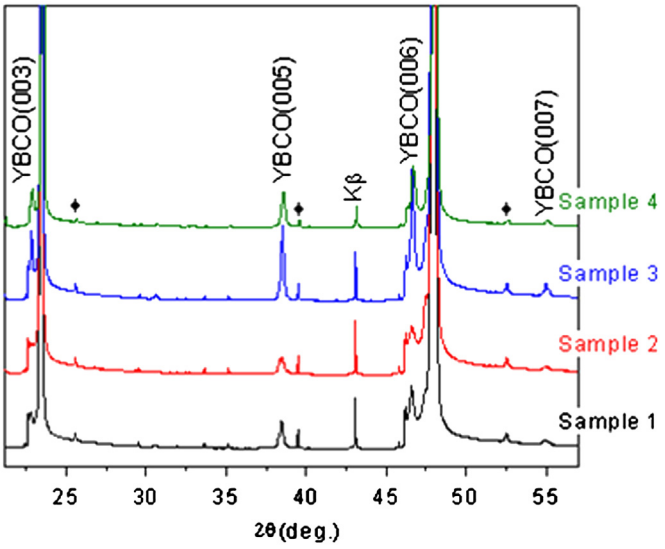

Fig. 7. XRD pattern of YBCO thin films. Sample 1: Precursor of pH=8.3, annealed at 790 °C for 1 h; Sample 2: Precursor of pH=6.5, annealed at 770 °C for 1 h; Sample 3: Precursor of pH=6.5, annealed at 790°C for 1 h; Precursor of pH=6.5, annealed at 810 °C for 1h. Peaks marked by ♦ are from background.

The extent of the complexation of the metal ions can be assessed by the FTIR spectra, as shown in Fig. 4. According to previous publications [17,18], vibrations in the wavenumber range from 800 to 400 cm^{-1} are due to Metal–O bonds. However, it is impossible to assign them here to a particular Metal–O bond because of the complexity of the precursor which contains three different metal cations. The broad peak at wavenumbers around 3000–3500 cm^{-1} is assigned to the vibration of O–H bonds in the sample, and the three peaks at 3016, 2925 and 2971 cm^{-1} are assigned to the C–H stretching

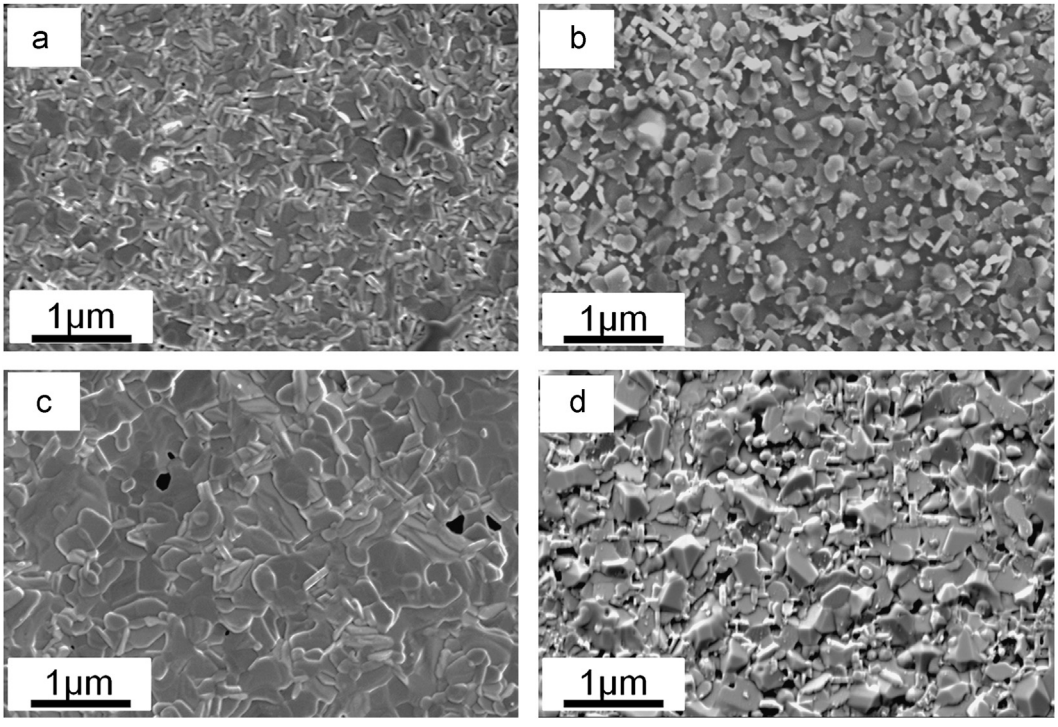

Fig. 8. Surface morphology (SEM) of YBCO thin films. Sample 1: Precursor with pH=8.3, annealed at 790 °C for 1 h; Sample 2: Precursor with pH=6.5, annealed at 770 °C for 1h; Sample 3: Precursor with pH=6.5, annealed at 790 °C for 1 h; Precursor with pH=6.5, annealed at 810 °C for 1 h.

vibrations of DEA. As most of the water had evaporated out from the gel, the O–H bonds originate primarily from the two $–CH_2CH_2OH$ branches of DEA. The spectra of the samples with pH values in the vicinity of 6.5 nearly coincide and have the lowest and the highest intensity levels in the ranges of 3000–3500 cm^{-1} and 600–700 cm^{-1}, respectively, implying a high tendency of Metal–O bond formation and the consumption of O–H bonds. However, the samples with the highest (8.3) or the lowest (5.6) pH values showed the converse behavior. Especially for the sample of pH=5.6, the O–H peak remains high, indicating little generation of Metal–O bonds. These observations correspond quite well to the expectation of $[M(H_2O)_n](AC)_z$ crystallization when no complexation with DEA occurs with the metal–organic salts.

Fig. 5 shows the morphology of pyrolyzed films derived from the precursors with pH=6.5 and pH=8.3 values respectively. The low-pH sample exhibits small particle size and distinct grain boundaries. In contrast, the high-pH sample shows a surface composed of much coarser particles and a roughness of 22.8 nm, which is almost two times that of the low-pH sample (14.8 nm). The morphology difference might originate from the different gelations processes that occur in the samples of different pH values [19,20].

In the low pH regime, the network formation is governed by the hydronium ion (H_3O^+), where the hydration rate is higher than the polymerization rate and thus olation takes place, as shown in Fig. 6. In this case straight linear chains are believed to form, which in consequence can induce the formation of small size particles after decomposition. Furthermore, under this mechanism the film coating and drying procedures can also benefit from the greater flexibility of the solution and large interstices of the gel, respectively. This can be observed with an optical microscope as seen in Fig. 2, where the gel sample of pH=6.5 shows a smooth surface, implying the release of stresses due to its higher flexibility. On the contrary, on the sample of pH=8.3, massive wrinkles are seen on the surface. Similar surface morphology was also observed on TFA-MOD derived samples by Dawley and was described as a "pencil-maze structure", which was believed to be harmful to thick film development via multilayering [21]. This is because in the high pH regime, the high concentration of hydroxyl (OH) leads to a vigorous polymerization process and thus entanglement among branched chains, which is the so-called oxolation. This will on the other hand lead to particle size enlargement, which hinders further solid state reaction during the sintering process. As in the annealing process, a typical solid reaction of the components $BaCO_3$, CuO and Y_2O_3 takes place. Theoretically, homogeneously distributed fine particles can enlarge the surface area [12] and shorten the diffusion paths [1]. This is advantageous for the formation of the YBCO superconducting phase at high temperature.

As high critical current density can only be achieved on epitaxially grown YBCO thin films, the samples were characterized by XRD measurements (Fig. 7). In sample 1, derived from the precursor with pH=8.3, though no peaks of secondary phases were detected, the intensity of the YBCO (00*l*) peaks were quite low, implying only a low amount of YBCO. From the SEM picture (Fig. 8a), it can be seen that the morphology of sample 1 is coarse and discontinuous. Some needle-like particles, probably *a*-axis oriented YBCO grains, were found agglomerating on some parts of the surface. Though too small to be observed in the XRD pattern, these randomly oriented grains can cause weak links, which

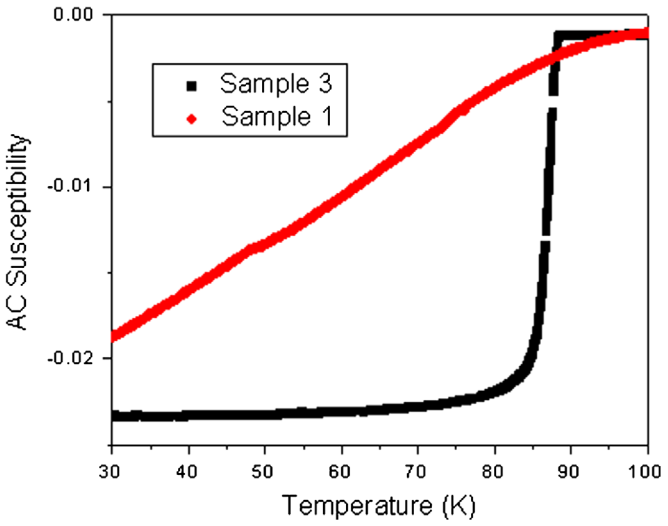

Fig. 10. Superconducting transition of sample1: Precursor of pH=8.3, annealed at 790 °C for 1 h; and Sample 3: Precursor of pH=6.5, annealed at 790 °C for 1 h.

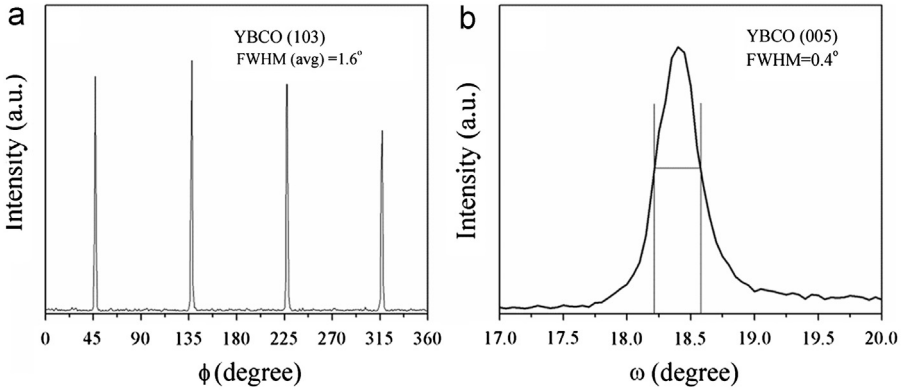

Fig. 9. (a) (103) Phi-scan of the sample 3; (b) (005) omega-scan of sample 3.

Table 2
Brief summary of the influence of initial pH value on YBCO products at different processing steps.

	Chelation	Polymerization	Pyrolysis	Annealing	Super conducting performance
pH = 5.6	Precipitation of acetates (High resistance)	×	×	×	×
6.0 < pH < 7.2	Homogeneous solution (Low resistance)	Olation (Straight chain)	Small particles	Good microstructure	$Jc = 0.1-0.2$ MA/cm^2
pH = 7.2	Homogeneous solution (High resistance)	Oxolation (entanglement)	Large particles	Bad microstructure	×

dramatically undermine the superconducting performance. By using the optimal solution (pH = 6.5) as the precursor, samples showed much better (00*l*) preferred growth orientation, except that annealed at the lower annealing temperature of 770 °C. The sample annealed at 790 °C exhibits the most intense YBCO (005) peak. Further increasing the annealing temperature to 810 °C results in a poorer texture. This is also reflected in the SEM pictures. From Fig. 8c, it is seen that sample 3 has a continuous and dense surface that is totally covered by flaky particles, indicating a preferential *c*-axis orientation.. In contrast, samples annealed at lower (sample 2) or higher (sample 4) temperatures showed porous and melt-like morphologies respectively, both of which are not promising for good superconducting performance.

Good out-of-plane and in-plane orientations of sample 3 are reflected by phi-scan and omega scan shown in Fig. 9, where the FWHM values are 0.4° and 1.6°, respectively. These results confirm that sample 3 has a superior microstructure compared to the others.

The AC susceptibility of the annealed YBCO samples was measured to characterize their superconducting behavior. The real component of the AC susceptibility of two samples between 30 K and 110 K are shown in Fig. 10. Obviously sample 3 displays a very sharp superconducting transition, which starts from 87.6 K, with a temperature width of less than 5 K. In contrast, sample 1 shows a sluggish transition, which is not complete until 30 K. Estimating the thickness to 150 nm and using the extended Bean critical state model, the critical current density (*Jc*) of sample 3 is approximately 0.25 MA/cm^2 at 77 K under self field, while the *Jc* of sample 1 is so low that it can be neglected. This result is well consistent with expectations based on the microstructural investigation.

4. Summary

In this report, an aqueous non-fluorine sol–gel method was successfully used to deposit YBCO superconducting thin films on LAO single crystals. DEA was used as a complexant to protect the metal ions from excessive hydrolysis. Solution conductivity was used as the indicator of the quality of the precursor solutions with different pH values. The effects of the pH value of precursor solution on the reaction behavior, final microstructure and superconducting performance are briefly summarized in Table 2. By optimizing the pH value of the starting solution, a homogeneous and well polymerized precursor was fabricated. After pyrolysis, fine particles were seen on the amorphous films, and following the annealing process, a *Jc* of 0.25 MA/cm^2 was obtained.

Acknowledgments

This work was supported by the Danish Agency for Science Technology and Innovation (Project nos 09-062997 and 09-065 234). The authors also acknowledge Dr N H Andersen from the Institute of Physics, Technical University of Denmark, for the hysteresis loops measurements.

References

[1] M. Kakihana, Invited review sol–gel preparation of high temperature superconducting oxides, Journal of Sol–Gel Science and Technology 6 (1996) 7–55, http://dx.doi.org/10.1007/BF00402588.

[2] K. Zalamova, A. Pomar, A. Palau, T. Puig, X. Obradors, Intermediate phase evolution in YBCO thin films grown by the TFA process, Superconductor Science and Technology 23 (2010) 014012, http://dx.doi.org/10.1088/0953-2048/23/1/014012.

[3] B.A. Glowacki, M. Mosiadz, The role of sol gel processing in the development of high temperature superconductors for AC applications, Journal of Sol–Gel Science and Technology 51 (2009) 335–347, http://dx.doi.org/10.1007/s10971-009-1980-8.

[4] D.L. Shi, Y.L. Xu, H.B. Yao, Z. Han, J. Lian, L.M. Wang, A.H. Li, H. K. Liu, S.X. Dou, The development of $YBa_2Cu_3O_x$ thin films using a fluorine-free sol–gel approach for coated conductors, Journal of Sol–Gel Science and Technology 17 (2004) 1420–1425, http://dx.doi.org/10.1088/0953-2048/17/12/011.

[5] K. Yamagiwa, T. Arakia, Y. Takahashia, H. Hieib, S.B. Kima, K. Matsumoto, J. Shibatad, T. Hirayamad, H. Ikutae, U. Mizutanib, I. Hirabayashi, Epitaxial growth of $REBa_2Cu_3O_{7-y}$ films on various substrates by chemical solution deposition, Journal of Crystal Growth 229 (2001) 353–357, http://dx.doi.org/10.1016/S0022-0248(01)01180-0.

[6] W. Cui, P. Mikheenko, L.M. Yu, T.W. Button, J.S. Abell, A. Crisan, $YBa_2Cu_3O_{7-x}$ thin films by citrate-based non-fluorine precursor, Journal of Superconductivity and Novel Magnetism 22 (2009) 811–815, http://dx.doi.org/10.1007/s10948-009-0504-7.

[7] T. Brylewski, K. Przybylski, Physicochemical property of high-Tc (Bi,Pb)–Sr–Ca–Cu–O and Y–Ba–Cu–O superconductors prepared by sol–gel technique, Applied Superconductivity 1 (1993) 737–744, http://dx.doi.org/10.1016/0964-1807(93)90283-8.

[8] W.T. Wang, G. Li, M.H. Pu, R.P. Sun, H.M. Zhou, Y. Zhang, H. Zhang, Y. Yang, C.H. Cheng, Chemical solution deposition of YBCO thin film by different polymer additives, Physica C 468 (2008) 1563–1566, http://dx.doi.org/10.1016/j.physc.2008.05.067.

[9] T.T. Tuy, S. Hoste, G.G. Herman, K. De Buysser, P. Lommens, J. Feys, D. Vandeput, I. Van Driessche, Sol–gel chemistry of an aqueous precursor solution for YBCO thin films, Journal of Sol–Gel Science and Technology 52 (2009) 124–133, http://dx.doi.org/10.1007/s10971-009-1987-1.

[10] G.V. Rama Rao, D.S. Suryanarayana, U.V. Varadaraju, T. Geetha Kumari, S. Venkadesan, Effect of pH on the synthesis of $YBa_2Cu_3O_7$ by the sol–gel process, Materials Chemistry and Physics 39 (1994) 149–156, http://dx.doi.org/10.1016/0254-0584(94)90192-9.

[11] P.K. Sharma, V.V. Varadan, A critical role of pH in the colloidal synthesis and phase transformation of nano size a-Al_2O_3 with high surface area, Journal of the European Ceramic Society 23 (2003) 659–666, http://dx.doi.org/10.1016/S0955-2219(02)00191-7.

[12] P.K. Shama, M.H. Jilavi, V.K. Varadan, H. Schmidt, Influence of initial pH on the particle size and fluorescence properties of the nano scale Eu (III) doped yttria, Journal of Physics and Chemistry of Solids 63 (2002) 171–177.

[13] E.M. Gyorgy, R.B. van Dover, K.A. Jackson, Anisotropic critical currents in $Ba_2YCu_3O_7$ analyzed using an extended Bean model, Applied Physics Letter 55 (1989) 283–285, http://dx.doi.org/10.1063/1.102387.

[14] J. Yang, W.J. Weng, Z.S. Ding, The drawing behavior of Y–Ba–Cu–O sol from non-aqueous solution by a complexing process, Journal of Sol–Gel Science and Technology 4 (1995) 187–193, http://dx.doi.org/10.1007/BF00488373.

[15] S. Grigoryan, A. Manukyan, A. Hayrapetyan, A. Arzumanyan, A. Kuzanyan, Y. Kafadaryan, E. Vardanyan, A new way of preparing the Y–Ba–Cu–O high-temperature superconductor using the sol–gel method, Superconductor Science and Technology 16 (2003) 1202–1206, http://dx.doi.org/10.1088/0953-2048/16/10/313.

[16] E.R. Savinova, A.L. Chuvilin, V.N. Parmon, Copper colloids stabilized by water-soluble polymers part 1. preparasion and properties, Journal of Molecular Catalysis 48 (1988) 217–229.

[17] M. Motta, C.V. Deimling, M.J. Saeki, P.N. Lisboa-Filho, Chelating agent effects in the synthesis of mesoscopic-size superconducting particles, Journal of Sol–Gel Science and Technology 46 (2008) 201–207, http://dx.doi.org/10.1007/s10971-007-1673-0.

[18] A. Baranauskas, D. Jasaitis, A. Kareiva, Characterization of sol–gel process in the Y–Ba–Cu–O acetate-tartrate system using IR spectroscopy, Vibrational Spectroscopy 28 (2002) 263–275, http://dx.doi.org/10.1016/S0924-2031(01)00157-6.

[19] E.J.A. Pope, J.D. Mackenzie, Sol–gel processing of silica: II. The role of the catalyst, Journal of Non-Crystalline Solids 87 (1986) 185–198, http://dx.doi.org/10.1016/S0022-3093(86)80078-3.

[20] Y.W. Chen, T.M. Yen, C.P. Li, Preparation of alumina–zirconia materials by the sol-gel method from metal alkoxides, Journal of Non-Crystalline Solids 185 (1995) 49–55, http://dx.doi.org/10.1016/0022-3093(94)00680-6.

[21] J.T. Dawley, P.G. Clem, M.P. Siegal, D.R. Tallant, D.L. Overmyer, Improving sol–gel $YBa_2Cu_3O_{7-\delta}$ film morphology using high-boiling-point solvents, Journal of Materials Research 17 (2002) 1900–1903, http://dx.doi.org/10.1557/JMR.2002.0282.